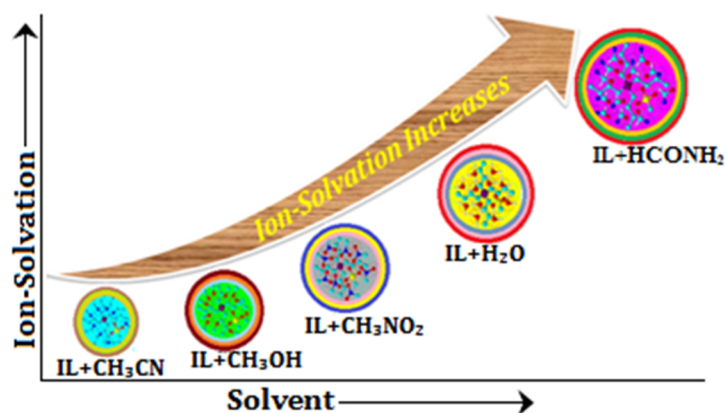


# CHAPTER-VI

## EXPLORATION OF SOLVATION CONSEQUENCE OF IONIC LIQUID $[Bu_4PCH_3SO_3]$ IN VARIOUS SOLVENT SYSTEMS BY CONDUCTANCE AND FTIR STUDY

Quantitative and qualitative analysis of molecular interactions prevailing in the ionic liquid tetrabutylphosphonium methanesulfonate  $[Bu_4PCH_3SO_3]$  in aqueous ( $H_2O$ ) and non-aqueous solvents, i.e., acetonitrile ( $CH_3CN$ ), methanol ( $CH_3OH$ ), nitromethane ( $CH_3NO_2$ ), and formamide ( $HCONH_2$ ) probed by precise measurements of electrical conductance ( $\lambda$ ) and FTIR spectroscopy respectively at 298.15K and atmospheric pressure.



The conductance data have been analyzed by the Fuoss conductance equation (1978) in terms of the limiting molar conductance ( $\lambda_0$ ), the association constant ( $K_A$ ), and the association diameter ( $R$ ) for ion-pair formation. The limiting ionic conductance ( $\lambda_0^\pm$ ) of the ions ( $Bu_4P^+$  and  $CH_3SO_3^-$ ) have been estimated from the appropriate division of limiting molar conductance of tetrabutylammonium tetrphenylborate  $[Bu_4NBPh_4]$  as "reference electrolyte" method along with a numerical evaluation of ion-pair formation constant. The molecular as well as ionic association have been discussed in terms of ion-dipole

interactions, H-bonding formation, structural aspect, and configurational theory. The FTIR spectroscopic studies of the variational intensity of characteristic functional group of the solvents have been undertaken and the solvation phenomenon is evident by the shifting of the band intensity in presence of the ionic liquid.

## **VI.1. INTRODUCTION**

In the past decade, ionic liquids (ILs) have been actively tested as innovative non volatile solvents and they are used in many academic and industrial research areas. Ionic liquids are good examples of neoteric solvents (new types of solvents, or older materials that are finding new applications as solvents), which is environmentally friendly (or eco-friendly) though some commonly used ionic liquids have a certain level of toxicity. Room-temperature ionic liquids (RTILs) are liquid salts with relatively low melting points (below 100°C) that usually consist of an organic cation or anion and a counter-ion. Generally, an ideal electrolyte should have high ionic conductivity ( $>10^{-4}$  S cm<sup>-1</sup>), fast ion mobility ( $>10^{-14}$  m<sup>2</sup> V<sup>-1</sup> s<sup>-1</sup>), large electrochemical potential windows ( $>1$  V), and low volatility. RTILs exhibit most of these properties and characteristics. Recently ionic liquids (ILs) have been considered as attractive compounds due to their unique intrinsic properties, such as negligible vapour pressure, large liquid range, ability of dissolving a variety of chemicals non-volatility, high thermal stability, large electrochemical window and their potential as 'designer solvents' and 'green' replacements for volatile organic solvents.<sup>VI.1</sup> Because of their unique properties, they are used as heat transfer fluids for processing biomass and electrically conductive liquids as electrochemical device in electrochemistry (batteries and solar cells),<sup>VI.2, VI.3</sup> and in reactions involving inorganic and bio-catalysis etc. The application

of the ionic liquids in the modern technology and electrochemistry is well understood by studying the ionic level of solvation the ions (ion-solvation or ion association) as well as by molecular solvation in the solution systems.

There are several imidazolium, pyridinium, ammonium and phosphonium based cation ionic liquids commercially available. Ionic liquids based on imidazolium cations have been demonstrated to exhibit high thermal stability than tetraalkylammonium, pyridinium based ionic liquids<sup>VI.4</sup> and are commercially available in large quantities.<sup>VI.5</sup> The substances with functional anionic group ( $[\text{CH}_3\text{SO}_3]^-$ ) are capable of additional interactions with polar solvents. The structure and diversity of functionality of the selected ionic liquid ( $[\text{Bu}_4\text{PCH}_3\text{SO}_3]$ ) have capable of most types of interactions (i.e., hydrogen bonding, dipolar, ionic/charge-charge, van der Waals forces etc).<sup>6,7</sup> The ion-pair formation was introduced by Bjerrum<sup>VI.8</sup> in 1926 and have been studied, primarily in solvents of high or medium dielectric constant ( $\epsilon_r > 12$ ), which has been taken into consideration for the calculation.

Subsequently, a quantity of conductometric<sup>VI.9</sup> and related studies of electrolytes in non-aqueous common solvents have been made for their optimal use in high-energy batteries<sup>VI.10</sup> and for further more understanding organic reaction mechanisms.<sup>VI.11</sup> Ionic association of electrolytes in solution depends upon the mode of solvation of its ions which in turn depends on the nature of the solvent/solvent mixtures. The solvent properties as viscosity and the relative permittivity have been taken into consideration as these properties help in determining the extent of ion association and the solvent-solvent interactions. The non-aqueous system has been of immense importance<sup>VI.12</sup> to the technologist and theoretician as many chemical processes occur in these systems to examine the nature and magnitude of ion-ion and ion-solvent interactions.

In continuation of our investigations on electrical conductance, in the present study, an attempt has been made to ascertain the nature of ion-association of ionic liquid (IL) tetrabutylphosphonium methanesulfonate [Bu<sub>4</sub>PMS] in aqueous (H<sub>2</sub>O) and non-aqueous polar protic/aprotic solvents, acetonitrile (CH<sub>3</sub>CN), methanol (CH<sub>3</sub>OH), nitromethane (CH<sub>3</sub>NO<sub>2</sub>), and formamide (HCONH<sub>2</sub>) as literature survey reveals that very scarce work has been carried out in studied binary solution systems. The solvation phenomenon is evident by the change of the variational intensity of characteristic bands in FTIR spectroscopy due to the presence of the [Bu<sub>4</sub>PMS].

## **VI.2. EXPERIMENTAL SECTION**

### **VI.2.1 Source and purity of materials**

The ionic liquid selected for the present work, tetrabutylphosphonium methanesulfonate [Bu<sub>4</sub>PMS] of puriss grade was procured from Sigma-Aldrich, Germany and used as purchased. The mass fraction purity of the ionic liquid is  $\geq 0.98$ .

The triply distilled water with a specific conductance  $< 1 \times 10^{-6} \text{ S cm}^{-1}$  at 298.15K and atmospheric pressure with mass fraction purity 0.999 (Table VI.1), was use for the experimental work.

All the solvents of spectroscopic grade were procured from Sigma-Aldrich, Germany and were used as purchased. The mass fraction purities of acetonitrile is 0.998, methanol is 0.998, nitromethane is 0.985, and formamide is 0.995 (Table VI.1). The purities of the solvents have been checked by measuring their densities, viscosities and conductivities, which were in good agreement with the literature values<sup>VI.13</sup> as shown in Table VI.2.

### **VI.2.2 Apparatus and Procedure**

All the stock solutions (0.1M) of the electrolyte (IL) were prepared by mass (weighted by Mettler Toledo AG-285 with uncertainty 0.0003g) in studied solvents. For conductance measurement the working solutions were obtained by mass dilution of the stock solutions.

The density of the solvents ( $\rho$ , g cm<sup>-3</sup>) were measured by means of vibrating u-tube Anton Paar digital density meter (DMA 4500M) with a precision of  $\pm 0.00005$  g cm<sup>-3</sup> maintained at  $\pm 0.01$  K of the desired temperature. It was calibrated by triply-distilled water and passing dry air.

Solvents viscosity ( $\eta$ , mPa s) were measured by means of suspended Ubbelohde type viscometer, calibrated with triply distilled water, purified methanol and dry air with dryer. A thoroughly cleaned and perfectly dried viscometer filled with experimental solution was placed vertically in a glass-walled thermostat (Bose Panda Instruments Pvt. Ltd.) maintained to  $\pm 0.01$  K of the desired temperature. After attaining thermal equilibrium, efflux times of flow were recorded with a stop watch. The flow times were accurate to  $\pm 0.1$  s. At least three repetitions of each data reproducible to  $\pm 0.1$  s were taken to average the flow times. Adequate precautions were taken to minimize evaporation losses during the actual measurements. Viscosity of the solvents is evaluated from recorded average flow time, using the following appropriate equation as described earlier.<sup>VI.14</sup> The uncertainty of the viscosity measurements was  $\pm 0.003$  mPa s.

The conductance measurements were carried out in a Systronics-308 conductivity bridge of accuracy  $\pm 1\%$ , using a dip-type immersion conductivity cell, CD-10 having a cell constant of approximately  $(0.1 \pm 0.001)$  cm<sup>-1</sup>. Measurements were made in a thermostat

water bath maintained at  $T = (298.15 \pm 0.01)$  K. The cell was calibrated by the method proposed by Lind et al.<sup>VI.15</sup> and cell constant was measured based on 0.01 M aqueous KCl solution. During the conductance measurements, cell constant was maintained within the range  $(1.10-1.12) \times 10^{-2} \text{ cm}^{-1}$ . The conductance data were reported at a frequency of 1 kHz and the accuracy was  $\pm 1\%$ . During all the measurements, uncertainty of temperatures was  $\pm 0.01$  K.

Infrared spectra were recorded in 8300 FTIR spectrometer (Shimadzu, Japan). The details of the instrument have already been previously described.<sup>VI.16</sup>

## VI.3. RESULTS AND DISCUSSION

### VI.3.1 Electrical Conductance

The selected ionic liquid (IL) was freely soluble in all proportions of the solvents. The physical properties of the solvents at 298.15 K are reported in Table VI.2.

The specific conductance ( $\kappa$ ,  $\mu\text{S cm}^{-1}$ ) of salt (IL) solutions under investigation with a molar concentration within the range of  $1.5 \times 10^{-5} - 1.0 \times 10^{-3}$  (M) in different solvents were measured. The molar conductances ( $\Lambda$ ,  $\text{S m}^2 \text{ mol}^{-1}$ ) for all studied solution system have been calculated using following equation.<sup>VI.17</sup>

$$\Lambda = 1000 \kappa / c \quad (1)$$

where  $c$  ( $\text{mol dm}^{-3}$ ) is the molar concentration and  $\kappa$  ( $\mu\text{S cm}^{-1}$ ) is the measured specific conductance of the studied solutions. The molar conductances ( $\Lambda$ ,  $\text{S m}^2 \text{ mol}^{-1}$ ) of the solutions of [Bu<sub>4</sub>PMS] in different studied solvents (IL+solvents) were calculated at the corresponding molar concentrations ( $c$ ,  $\text{mol dm}^{-3}$ ) and given in Table VI.3. For all the chosen solvents in higher and moderate relative permittivity ( $\epsilon_r > 12$ ), as in water ( $\epsilon_r =$

78.30), acetonitrile ( $\epsilon_r = 35.95$ ), methanol ( $\epsilon_r = 32.70$ ), nitromethane ( $\epsilon_r = 35.87$ ), and formamide ( $\epsilon_r = 109.50$ ), the conductance curves ( $\Lambda$  versus  $\sqrt{c}$ ) for the ionic liquid were found to be linear and depicted in Figure VI.1. Thus the conductance data in studied solvents systems have been analyzed using the Fuoss conductance equation.<sup>VI.18, VI.19</sup> For a given set of conductivity values ( $c_j, \Lambda_j, j=1, \dots, n$ ), three adjustable parameters, the limiting molar conductance ( $\Lambda_0, S \text{ m}^2 \text{ mol}^{-1}$ ) the association constant ( $K_A, \text{dm}^3 \text{ mol}^{-1}$ ) and the distance of closest approach of ions ( $R, \text{\AA}$ ) are derived from the following set of equations

$$\Lambda = P\Lambda_0[(1 + R_x) + E_L] \quad (2)$$

$$P = 1 - \alpha(1 - \gamma) \quad (3)$$

$$\gamma = 1 - K_A c \gamma^2 f^2 \quad (4)$$

$$-\ln f = \beta \kappa / 2(1 + \kappa R) \quad (5)$$

$$\beta = e^2 / (\epsilon_r k_B T) \quad (6)$$

$$K_A = K_R / (1 - \alpha) = K_S / (1 + K_S) \quad (7)$$

where  $R_x$  is the relaxation field effect,  $E_L$  (amp) is the electrophoretic counter current,  $k^{-1}$  ( $\kappa, \text{\AA}$ ) is the radius of the ionic atmosphere,  $\epsilon_r$  is the relative permittivity of the solvents,  $e$  (C) is the electron charge,  $c$  ( $\text{mol dm}^{-3}$ ) is the molarity of the solution,  $k_B$  ( $\text{J K}^{-1}$ ) is the Boltzmann constant,  $K_A$  ( $\text{dm}^3 \text{ mol}^{-1}$ ) is the overall pairing constant,  $K_S$  ( $\text{dm}^3 \text{ mol}^{-1}$ ) is the association constant of the contact-pairs,  $K_R$  ( $\text{dm}^3 \text{ mol}^{-1}$ ) is the association constant of the solvent-separated pairs,  $\gamma$  is the fraction of solute present as unpaired ion,  $\alpha$  is the fraction of contact pairs,  $f$  is the activity coefficient,  $T$  (K) is the absolute temperature and  $\beta$  ( $\text{\AA}$ ) is twice the Bjerrum distance. The computations were performed using a program suggested by Fuoss<sup>VI.19</sup>. The initial  $\Lambda_0$  ( $S \text{ m}^2 \text{ mol}^{-1}$ ), values for the iteration procedure were obtained from Shedlovsky extrapolation of the data. Input for the program is the set

( $c_j, \Lambda_j, j = 1, \dots, n$ ),  $n, \epsilon_r, \eta$  ( $\text{mPa s}^{-1}$ ),  $T$  (K), initial values of  $\Lambda_0$  ( $\text{S m}^2 \text{mol}^{-1}$ ), and an instruction to cover a pre-selected range of ( $R, \text{\AA}$ ) values.

The best value of a parameter is the one when equations is best fitted to the experimental data corresponding to minimum standard deviation  $\delta$  for a sequence of predetermined  $R, (\text{\AA})$  values, and standard deviation  $\delta$  was calculated by the following equation

$$\delta^2 = \sum_{j=1}^n [\Lambda_j(\text{cal}) - \Lambda_j(\text{obs})]^2 / (n - m) \quad (8)$$

where  $n$  is the number of experimental points and  $m$  is the number of fitting parameters. The conductance data were analyzed by fixing the distance of closest approach  $R$  with two parameter fit ( $m = 2$ ). As for the studied electrolyte (IL) in various solvents (water, acetonitrile, methanol, nitromethane, formamide), no significant minima were observed in the  $\delta$  versus  $R$  ( $\text{\AA}$ ) curves, whereas the  $R$  ( $\text{\AA}$ ) values were arbitrarily preset at the centre to centre distance of solvent-separated ion pair. Thus,  $R$  ( $\text{\AA}$ ) values are assumed to be

$$R = a + d \quad (9)$$

where  $a = (r_+ + r_-)$  is the sum of the crystallographic radii of the cation ( $r_+, \text{\AA}$ ) and anion ( $r_-, \text{\AA}$ ) and  $d$  ( $\text{\AA}$ ) is the average distance corresponding to the side of a cell occupied by a solvent molecule. The distance,  $d$  ( $\text{\AA}$ ) is given by<sup>VI.20</sup>

$$d (\text{\AA}) = 1.183 (M / \rho)^{1/3} \quad (10)$$

where  $M$  ( $\text{g mol}^{-1}$ ) and  $\rho$  ( $\text{kg m}^{-3}$ ) is the molar mass and density of the solvents respectively. The values of  $\Lambda_0$  ( $\text{S m}^2 \text{mol}^{-1}$ ),  $K_A$  ( $\text{dm}^3 \text{mol}^{-1}$ ), and  $R$  ( $\text{\AA}$ ) obtained by this procedure are represented in Table VI.4. Perusal of Table VI.4 and Figure VI.2 reveals that the limiting

molar conductances ( $\Lambda_0$ , S m<sup>2</sup> mol<sup>-1</sup>) for the electrolyte (IL) gradually decrease from acetonitrile to formamide of the studied solvents, as following trend:<sup>VI.21</sup>

acetonitrile > methanol > nitromethane > water > formamide

The Table also reveals that the association constant of the [Bu<sub>4</sub>PMS] is opposite of the limiting molar conductances, lower in acetonitrile and higher in formamide, which is in order;

HCONH<sub>2</sub> > H<sub>2</sub>O > CH<sub>3</sub>NO<sub>2</sub> > CH<sub>3</sub>OH > CH<sub>3</sub>CN

Hence the ion-solvent interaction or ion-association increases from acetonitrile to formamide among the chosen solvents, leading to a lower conductance of [Bu<sub>4</sub>PMS]. From the Table VI.2 and VI.4, we can support the above facts from the viscosity values, as following; the limiting molar conductances for the ionic liquid in chosen solvents are linearly vary with reciprocal of the solvent viscosity ( $1/\eta$ ) (or fluidity,  $\eta^{-1}$ , (mP s)<sup>-1</sup>), i.e.; the electrolyte (IL) in the lower viscous solvent, the  $\Lambda_0$  (S m<sup>2</sup> mol<sup>-1</sup>) value should increase.<sup>VI.13, VI.22</sup> But the conductance data randomly vary with the relative permittivity of the solvents. Thus if we consider the effect of solvent properties (as viscosity and relative permittivity), the variation of conductance data depends upon the viscosity values of the solvents rather than the relative permittivity, which suggested that the solvents viscosity ( $\eta$ , mP s) is predominant over the relative permittivity ( $\epsilon_r$ ), in effecting the electrolytic conductance of the electrolyte (IL) under the studied solution media.

The trend in  $\Lambda_0$  and ion-association can also be discussed through another characteristic function called the Walden product ( $\Lambda_0\eta$ , S m<sup>2</sup> mol<sup>-1</sup> mP s) (which is the product of limiting molar conductance and solvent viscosity) and it is a constant under normal condition, given in Table VI.4. Table VI.4 and Figure VI.3 of the plot of Walden

product vs. the solvent type show that, the arbitrarily decrease the Walden product from acetonitrile to water and then sharply increases in formamide. The decreasing trend is in accordance with the concomitant increase of viscosity and decreasing limiting molar conductance of the electrolyte (IL) in the solvents, but the sharp increase in case of formamide is obviously due to the sharply increase in viscosity value or the effect of the high viscosity. This is justified as the Walden product of an ion or solute is inversely proportional to the effective solvated radius,  $r_{\text{eff}}$ , (Å) of the ion or solute in a particular solvent/solvent mixture. VI.23

$$\Lambda_0 \eta = \frac{1}{6\pi r_{\text{eff}} T} \quad (11)$$

This points out to the fact that the electrostatic ion-solvent interaction or ion-association is strong in these cases. The variation of the Walden product reflects the change of salvation.

VI.24

The solvation of molecule (ionic liquid) as well as ions in the chosen solvents can be explain by

(i) Preference to solvation of ionic liquid for solvents molecules:

Taking consideration of the conductance and association constant value of ionic liquids in different solvents, we can say that the IL mostly prefers the formamide among the solvents and the order of preference by the IL is as follows:

formamide > water > nitromethane > methanol > acetonitrile

(ii) With considering the structural aspect of the solvents:

(a) In case of acetonitrile (CH<sub>3</sub>CN), the only interaction present between negatively charged nitrogen atom of acetonitrile and positively charged P atom of [Bu<sub>4</sub>P]<sup>+</sup>,

shown in (I) of **Scheme VI.1**. Dimerization of acetonitrile, in  $\text{CH}_3\text{C}^+\text{N}^-$  most of the positive charge is on the nitrile carbon, *i.e.*, "inside" the molecule, evidence that acetonitrile tends to associate and forming the antiparallel dimer<sup>VI.25</sup> **Scheme VI.2**. The existence of antiparallel dimerization in acetonitrile, leads to the formation of less ion-solvent interaction.

- (b) Same type of interaction is present in case of solvent methanol, shown in (II), where the interaction is more intense due to the presence of more negative oxygen atom, making it stronger interaction with IL.
- (c) In case of nitromethane, where the two electronegative oxygen atoms present with nitrogen, resulting in more ion-solvent interaction, shown in (III).
- (d) In aqueous solution of ionic liquid, the smaller in size and shape, having higher power of penetration effect, presence of very high electronegative oxygen atom with loosely bounded lone pair of electron, having very efficient to form H-bonding the water molecules strongly interact with the ions of ionic liquid, resulting in greater ion-association, shown in (IV).
- (e) From the structure of formamide there are three possibilities of interaction as with N-H, C=O, C-H bonds. Thus in the solution of IL+formamide, the formamide strongly interact with the ionic liquid with H-bond/ion-dipole and above mentioned bonds. Hence gives the highest value of ion-association as well as higher aggregation.

Hence, lower is the conductance, more the ion-solvent interaction/ion-association. The ion-association is in the following order-



The schematic representation of plausible ion-solvent interaction, for the particular ion in the studied solutions (i.e; [Bu<sub>4</sub>PMS]<sup>+</sup>+solvents), in view of various derived parameters is depicted in **Scheme VI.1**.

The starting point for most evaluations of ionic conductance is Stokes' law which states that the limiting ionic Walden product ( $\lambda_0^{\pm}\eta$ , S m<sup>2</sup> mol<sup>-1</sup> mP s) (the product of the limiting ionic conductance and solvent viscosity) for any singly charged, spherical ion is a function only of the ionic radius and thus under normal conditions, is a constant. The ionic conductances  $\lambda_0^{\pm}$  (S m<sup>2</sup> mol<sup>-1</sup>) (for the Bu<sub>4</sub>P<sup>+</sup> cation and MS<sup>-</sup> anion) in different solvents, were calculated using tetrabutylammonium tetraphenylborate (Bu<sub>4</sub>NBPh<sub>4</sub>) as a 'reference electrolyte' following the scheme as suggested by B. Das et al.<sup>VI.26</sup> We have calculated the limiting ionic conductances  $\lambda_0^{\pm}$  (S m<sup>2</sup> mol<sup>-1</sup>) in our solvent compositions by interpolation of conductance data from the literature<sup>VI.27</sup> using cubic spline fitting. The ionic conductance values given in Table VI.5 and Figure VI.2 shows that the greater share of the conductance value comes for the anion MS<sup>-</sup> than the cation [Bu<sub>4</sub>P]<sup>+</sup>. The Table VI.5 and Figure VI.2 shows that the contribution of ionic conductance values also decrease from acetonitrile to formamide for the studied ionic liquid (IL).

The  $\lambda_0^{\pm}$  (S m<sup>2</sup> mol<sup>-1</sup>) values were in turn utilized for the calculation of Stokes' radii ( $r_s$ , Å) according to the classical expression.<sup>VI.28</sup>

$$r_s = \frac{F^2}{6\pi N_A \lambda_0^{\pm} r_c} \quad (12)$$

Ionic Walden products  $\lambda_0^{\pm}\eta$  (S m<sup>2</sup> mol<sup>-1</sup> mP s), Stokes' radii  $r_s$  (Å), and crystallographic radii  $r_c$  (Å) are presented in Table VI.5. The trends in Walden products  $\lambda_0\eta$  and ionic Walden products  $\lambda_0^{\pm}\eta$  for the electrolyte in the solvents are depicted in Table VI.4

and VI.5 respectively and in Figure VI.3. It shows that both the ionic Walden products  $\lambda_{o^{\pm}}\eta$  and Walden products  $\Lambda_{o^{\pm}}\eta$  vs. the solvent type for the electrolyte randomly decreases from acetonitrile to water and then increase sharply in formamide. For  $\text{Bu}_4\text{P}^+$  and  $\text{MS}^-$  ion, the Stokes' radii  $r_s$  (Å) are either lower or comparable to their crystallographic radii  $r_c$  (Å), this suggests that the ion are comparatively less solvated than alkali metal ions due to its intrinsic low surface charge density. The distance parameter  $R$  (Å), shown in Table VI.4, is the least distance that two free ions can approach before they merge into an ion-pair.

The nature of the curve for the Gibb's energy changes for ion-pair formation,  $\Delta G^\circ$  (kJ mol<sup>-1</sup>) clearly predicts the tendency for ion-pair formation. The Gibb's energy change  $\Delta G^\circ$  (kJ mol<sup>-1</sup>) is given by the following relationship<sup>VI.29</sup> and is given in Table VI.4.

$$\Delta G^\circ = - RT \ln K_A \quad (13)$$

The negative values of  $\Delta G^\circ$  (kJ mol<sup>-1</sup>) can be explained by considering the participation of specific interaction in the ion-association process. It is observed from the Table VI.4 that the values of the Gibb's free energy are all negative, entire all over the solutions and the negativity increases from acetonitrile to formamide. The increasing negativity in the value of  $\Delta G^\circ$  (kJ mol<sup>-1</sup>) of  $[\text{Bu}_4\text{PMS}]$  leads to the increase in the ion-solvent interaction. This result indicates the extent of solvation enhanced by the following order:



This is an excellent agreement with the observation obtained from conductance values discussed earlier in this paper.

There are marked characteristic behaviours in the association constant ( $K_A$ , dm<sup>3</sup> mol<sup>-1</sup>) values, which generally increase from acetonitrile to formamide; the thermal motion

probably destroys the solvent structure. However, from the Table VI.4, ion-association for the electrolyte (IL) increases from acetonitrile to formamide among the studied solvents.

The diffusion coefficient ( $D_{\pm}$ ,  $\text{m}^2 \text{s}^{-1}$ ) is obtained using the Stokes-Einstein Relation

$$D_{\pm} = \frac{k_B T}{6\pi\eta r_s} \quad (14)$$

where  $k_B$  ( $\text{J K}^{-1}$ ) is the Boltzmann's constant,  $T$  (K) is the temperature,  $\eta$  ( $\text{mP s}$ ) is the solvent viscosity and  $r_s$  ( $\text{\AA}$ ) is the Stoke's radii.

The ionic mobility ( $i_{\pm}$ ,  $\text{m}^2 \text{s}^{-1} \text{ volt}^{-1}$ ) was obtained using the following equation

$$i_{\pm} = \frac{z_{\pm} F}{R_g T} D_{\pm} \quad (15)$$

where  $z_{\pm}$ ,  $F$  ( $\text{C mol}^{-1}$ ),  $R_g$  ( $\text{J K}^{-1} \text{ mol}^{-1}$ ),  $T$  (K) and  $D_{\pm}$  ( $\text{m}^2 \text{s}^{-1}$ ) is the ionic charge, Faraday constant, universal gas constant, temperature, and diffusion coefficient respectively. Diffusion coefficient ( $D_{\pm}$ ,  $\text{m}^2 \text{s}^{-1}$ ) and ionic mobility ( $i_{\pm}$ ,  $\text{m}^2 \text{s}^{-1} \text{ volt}^{-1}$ ) for both the ion ( $\text{Bu}_4\text{P}^+$  and  $\text{MS}^-$ ) in the studied solvents is given in Table VI.6. Table VI.6 shows that the contribution of diffusion coefficient of the anion  $\text{MS}^-$  is more than the cation  $\text{Bu}_4\text{P}^+$  in all the studied solvents which indicates that  $\text{MS}^-$  ion diffuses more through the solvents. The diffusion coefficient decrease from acetonitrile to formamide as indicated in Table VI.6, for both  $\text{Bu}_4\text{P}^+$  and  $\text{MS}^-$  ions showing greater diffusion of the ions in acetonitrile. At the same time the ionic mobility value given in Table VI.6 also shows that the mobility of  $\text{MS}^-$  is higher than  $\text{Bu}_4\text{P}^+$  in all the investigated solvents, indicating greater share of conductance by  $\text{MS}^-$  mentioned earlier i.e.; the diffusion coefficient is directly proportional to the ionic mobility and these are the driving force to conduct electricity by IL or ions in solutions. From the same table we have seen that the mobility of both the ions decrease from acetonitrile to formamide. This is due to the fact that the increase in the viscosity of the

solvent as well as the increase in the ion-solvent interaction or ion-solvation, which is evident from the association constant values, reported in Table VI.4.

### **VI.3.2 FTIR Spectroscopic Study**

With the help of FTIR spectroscopy the molecular interaction existing between the ionic liquid and the solvents have been presented qualitatively and used as supportive evidence for the study of bond formation due ion-solvent and solvent-solvent interactions. The IR spectra of the pure solvents and studied solutions of {[Bu<sub>4</sub>PMS]<sup>+</sup>Solvent} have been studied. The stretching frequencies of the functional groups of solvents and shifting in frequencies of the functional groups when ionic liquid mixed are given in Table VI.7 and Figure VI.4-VI.8 within the range of wave number 400-4000 cm<sup>-1</sup>. The concentration of the studied solutions used in the IR study is 0.05 M.

The IR spectra of acetonitrile show a sharp peak at  $\nu_o = 2255.6 \text{ cm}^{-1}$  which is attributed to the C≡N stretching vibration range (2210-2260 cm<sup>-1</sup>). The peak shifted to  $\nu_s = 2289.4 \text{ cm}^{-1}$  when the electrolyte (IL) is added to acetonitrile (i.e., [Bu<sub>4</sub>PMS]<sup>+</sup>CH<sub>3</sub>CN). This is due to the disruption of dipole-dipole interaction present in acetonitrile<sup>VI.26</sup> leading to the formation of ion-dipole interaction between [Bu<sub>4</sub>P]<sup>+</sup> ion with C≡N bond leading to the shift in the C≡N stretching frequency. Shift in stretching frequency of C-H bond of CH<sub>3</sub>CN is negligible ( $\Delta\nu=3.4 \text{ cm}^{-1}$ ), which shows that C-H bond does not contribute in the interaction.

In case of methanol, a broad peak is obtained at  $\nu_o = 3384.7 \text{ cm}^{-1}$  which is attributed to H-bonded O-H stretching vibration (within the range 3200-3600 cm<sup>-1</sup>). But when the IR spectra of [Bu<sub>4</sub>PMS]<sup>+</sup>CH<sub>3</sub>OH solution was taken, the broad peak shifted to  $\nu_s = 3426.6 \text{ cm}^{-1}$  and it was a bit narrower than that obtained in case of pure methanol. This indicates that

the H-bonding existing between the methanol molecules<sup>VI.30</sup> is disrupted by the addition of the [Bu<sub>4</sub>PMS]. This may be due to the interaction of ions [Bu<sub>4</sub>P]<sup>+</sup> or MS<sup>-</sup> with the -OH of CH<sub>3</sub>OH leading to the shift in the H-bonded O-H stretching frequency. Negligible change in stretching frequency of C-H bond ( $\Delta\nu = 3.4 \text{ cm}^{-1}$ ) of CH<sub>3</sub>OH shows interaction does not occurred.

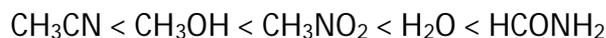
In case of nitromethane, two bands are obtained in the regions  $\nu_o = 1565.3 \text{ cm}^{-1}$  and  $1363.8 \text{ cm}^{-1}$ , former for the asymmetric stretching vibration ( $\nu_{as}$ ) of N-O ( $1500\text{-}1570 \text{ cm}^{-1}$ ) and the latter for symmetric stretching vibration ( $\nu_s$ ) of N-O ( $1300\text{-}1370 \text{ cm}^{-1}$ ) respectively shown in Table VI.7. The C-H stretching frequency of the -CH<sub>3</sub> group in CH<sub>3</sub>NO<sub>2</sub> occurs at  $2963.0 \text{ cm}^{-1}$  attributing to  $\nu_{as}$  of C-H and  $2872.9 \text{ cm}^{-1}$  attributing to  $\nu_s$  of C-H. By the addition of [Bu<sub>4</sub>PMS] in CH<sub>3</sub>NO<sub>2</sub>, the  $\nu_{as}$  of N-O shifts from  $1565.3 \text{ cm}^{-1}$  to  $1617.9 \text{ cm}^{-1}$  and  $\nu_s$  of N-O shifts from  $1363.8 \text{ cm}^{-1}$  to  $1414.8 \text{ cm}^{-1}$  which is reported in Table VI.7. The shift in the bands may be due to the rupture of the H-bonding interaction present in the CH<sub>3</sub>NO<sub>2</sub> molecules.<sup>VI.31</sup> The electrolyte and the solvent molecules interact via ion-dipole interaction. Negligible change in stretching frequency of C-H bond ( $\Delta\nu = 0.6 \text{ cm}^{-1}$ ) of CH<sub>3</sub>NO<sub>2</sub>, shows the interaction is absent between C-H and IL.

Similarly, in water two bands are obtained in the regions  $\nu_o = 3449.2 \text{ cm}^{-1}$  and  $3344.6 \text{ cm}^{-1}$ , former for the asymmetric stretching vibration ( $\nu_{as}$ ) and the latter for symmetric stretching vibration ( $\nu_s$ ) of O-H respectively within the range ( $3100\text{-}3800 \text{ cm}^{-1}$ ) presented in Table VI.7. When [Bu<sub>4</sub>PMS] was added in aqueous solution, the asymmetric stretching frequency ( $\nu_{as}$ ) and symmetric stretching frequency ( $\nu_s$ ) of O-H got shifted to  $3514.8 \text{ cm}^{-1}$  and  $3405.1 \text{ cm}^{-1}$  respectively which is also reported in Table VI.7. We know that the H-bonding interaction is present in H<sub>2</sub>O.<sup>VI.32</sup> The shift in the both bands may be due

to the rupture of the H-bonding interaction between the H<sub>2</sub>O molecules and the electrolyte interact via ion-dipole interaction of ions [Bu<sub>4</sub>P]<sup>+</sup> /MS<sup>-</sup> with the -OH of H<sub>2</sub>O leading to the shift in the H-bonded O-H stretching frequency.

In case of formamide, the bands are obtained in the regions  $\nu_0 = 1578.7 \text{ cm}^{-1}$ ,  $1693.4 \text{ cm}^{-1}$  and  $1402.0 \text{ cm}^{-1}$  for N-H ( $1500\text{-}1600 \text{ cm}^{-1}$ ), C=O ( $1650\text{-}1695 \text{ cm}^{-1}$ ), and C-N ( $\sim 1400 \text{ cm}^{-1}$ ) respectively and given in Table 7. The peaks shifts to  $\nu_s = 1589.9 \text{ cm}^{-1}$ ,  $1782.6 \text{ cm}^{-1}$  and  $1403.5 \text{ cm}^{-1}$  for N-H, C=O, and C-N respectively when the electrolyte (IL) is added to formamide (i.e; [Bu<sub>4</sub>PMS]<sup>+</sup> HCONH<sub>2</sub>). This is due to the disruption of dipole-dipole interaction present in formamide <sup>VI.32</sup> leading to the formation of ion-dipole interaction between the ion [Bu<sub>4</sub>P]<sup>+</sup>/MS<sup>-</sup> with N-H, C=O bond leading to the shifting of the stretching frequency of these bonds. The change in stretching frequency for C-N, N-H, and C=O is  $\Delta\nu = 1.5, 11.2, \text{ and } 89.2 \text{ cm}^{-1}$ , respectively indicates that the contribution of C=O, play a vital role in the interaction with the electrolyte than other two.

Table VI.7 also reveal that the  $\Delta\nu \text{ (cm}^{-1}\text{)}$  values increases from acetonitrile to formamide under investigation, i.e. the shifting in stretching frequency increases from acetonitrile to formamide solution. The order of  $\Delta\nu \text{ (cm}^{-1}\text{)}$  from the FTIR spectra is



Higher in the change in stretching frequency for the functional group from solvent to solution ( $\Delta\nu, \text{ cm}^{-1}$ ) greater is the pulling effect of solvent molecules by ionic liquid (IL) as well as by ions toward itself and resulting in greater ion-solvation. Increasing  $\Delta\nu \text{ (cm}^{-1}\text{)}$  values from acetonitrile to formamide shows the ion-solvent interaction increases. This is in compliance with the data obtained in the conductivity study discussed earlier, which shows that there is more association between the IL and the solvent molecules.

A schematic representation of the interaction occurring in pure solvents and {[Bu<sub>4</sub>PMS]+Solvents} together with the trend in the ion-solvation in the studied solvents has been shown in **Scheme VI.3**.

## **VI.4. CONCLUSION**

The present work reveals an extensive study on the ion-solvation behaviour of the tetrabutylphosphonium methanesulfonate [Bu<sub>4</sub>PMS] in industrially important polar protic aqueous (H<sub>2</sub>O) and non-aqueous solvents acetonitrile (CH<sub>3</sub>CN), methanol (CH<sub>3</sub>OH), nitromethane (CH<sub>3</sub>NO<sub>2</sub>), and formamide (HCONH<sub>2</sub>), through the conductometric and FTIR measurements. It becomes clear that the electrolyte (IL) exists as ion-pair in all the studied solutions. The tendency of the ion-pair depends on the size the charge distribution of the ions, and structural aspects (functional group of the solvents). The diffusion coefficient and the ionic mobility decrease from acetonitrile to formamide for both the [Bu<sub>4</sub>P]<sup>+</sup> and MS<sup>-</sup> ions showing greater ion-solvent interaction in formamide than the other studied solvents. In all the solvents the electrolyte forms ion-dipole interactions as evident from the FTIR studies. The derived parameters obtained by analyzing various equations supplemented with experimental data sustain the same finale as discussed and explained in this manuscript demanding the uniqueness of the work.

## TABLES

Table VI.1: Sample description

Chemicals name	Source	Purification method	Mass fraction purity
[Bu <sub>4</sub> PCH <sub>3</sub> SO <sub>3</sub> ]	Sigma-Aldrich, Germany	Used as procured	0.980
CH <sub>3</sub> CN	Sigma-Aldrich, Germany	Used as procured	0.998
CH <sub>3</sub> OH	Sigma-Aldrich, Germany	Used as procured	0.998
CH <sub>3</sub> NO <sub>2</sub>	Sigma-Aldrich, Germany	Used as procured	0.985
H <sub>2</sub> O	Laboratory	Fractional Distillation Method	0.999
HCONH <sub>2</sub>	Sigma-Aldrich, Germany	Used as procured	0.995

Table VI.2: Values of density ( $\rho$ ), viscosity ( $\eta$ ) and relative permittivity ( $\epsilon_r$ ) at  $T = 298.15$  K and pressure  $p = 101.325$  kPa of studied pure solvents<sup>a</sup>

Solvents	$\rho \times 10^{-3}(\text{kg m}^{-3})$		$\eta$ (mPa s)		$\epsilon_r$
	Expt	Lit	Expt	Lit	
CH <sub>3</sub> CN	0.77668	0.77667 <sup>34</sup>	0.344	0.3446 <sup>34</sup>	35.95 <sup>13</sup>
CH <sub>3</sub> OH	0.78661	0.78660 <sup>13</sup>	0.546	0.545 <sup>13</sup>	32.70 <sup>13</sup>
CH <sub>3</sub> NO <sub>2</sub>	1.13015	1.13015 <sup>14</sup>	0.615	0.614 <sup>14</sup>	35.87 <sup>14</sup>
H <sub>2</sub> O	0.99712	0.99710 <sup>13</sup>	0.891	0.890 <sup>13</sup>	78.30 <sup>13</sup>
HCONH <sub>2</sub>	1.12922	1.12920 <sup>13</sup>	3.303	3.302 <sup>13</sup>	109.50 <sup>13</sup>

<sup>a</sup>standard uncertainties  $u$  are  $u(\rho) = 0.00005$  g cm<sup>-3</sup>,  $u(\eta) = 0.003$  mPa s,  $u(T) = 0.01$  K, and  $u(p) = 10$  kPa.

**Table VI.3: Molar conductance ( $\Lambda$ ) and the corresponding concentration ( $m$ ) of [Bu<sub>4</sub>PMS] at  $T = 298.15$  K and pressure  $p = 101.325$  kPa in different studied solvents<sup>a</sup>**

$c \times 10^4$ (mol dm <sup>-3</sup> )	$\Lambda \times 10^4$ (S m <sup>2</sup> mol <sup>-1</sup> )	$c \times 10^4$ (mol dm <sup>-3</sup> )	$\Lambda \times 10^4$ (S m <sup>2</sup> mol <sup>-1</sup> )	$c \times 10^4$ (mol dm <sup>-3</sup> )	$\Lambda \times 10^4$ (S m <sup>2</sup> mol <sup>-1</sup> )
CH <sub>3</sub> CN		CH <sub>3</sub> OH		CH <sub>3</sub> NO <sub>2</sub>	
9.62	158.92	9.00	82.64	8.53	76.49
17.64	156.01	14.38	79.33	13.18	74.08
24.42	154.09	19.91	76.86	17.64	72.31
30.24	152.66	24.65	75.21	24.01	69.80
35.28	151.34	29.38	73.67	29.70	67.42
39.68	150.32	35.88	72.08	36.12	65.33
47.03	148.92	42.38	70.03	41.86	63.04
52.91	147.60	49.14	68.62	49.14	61.06
61.73	146.11	57.46	66.00	57.00	58.81
71.69	144.53	67.08	64.45	66.10	56.34
80.63	143.20	77.79	61.99	76.04	54.06
87.58	142.18	86.49	60.29	85.93	51.80
H <sub>2</sub> O		HCONH <sub>2</sub>			
8.07	41.19	8.29	21.52		
14.52	38.77	14.52	20.07		
20.25	36.65	20.25	18.60		
26.32	34.79	26.32	17.66		

31.81	33.44	31.81	16.72
37.82	31.68	37.82	15.93
45.70	30.04	45.70	14.76
52.91	28.79	52.91	13.91
61.31	27.36	61.31	12.97
70.56	25.77	70.56	11.94
79.21	24.50	79.21	11.32
84.82	23.97	84.82	10.70

<sup>a</sup>standard uncertainties  $u$  are  $u(m) = 2 \times 10^{-6} \text{ mol dm}^{-3}$ , and  $u(\Lambda) = 1 \times 10^{-6} \text{ S m}^2 \text{ mol}^{-1}$ ,  $u(T) = 0.01 \text{ K}$ , and  $u(p) = 10 \text{ kPa}$ .

**Table VI.4: Limiting molar conductivity ( $\Lambda_0$ ), the association constant ( $K_A$ ), the distance of closest approach of ions ( $R$ ), standard deviations  $\delta$  of experimental  $\Lambda$  from equation 1, Walden product ( $\Lambda_0\eta$ ) and Gibb's energy change ( $\Delta G^0$ ) of [Bu<sub>4</sub>PMS] in different studied solvents at  $T = 298.15 \text{ K}$**

Solvents	$\Lambda_0 \times 10^4$ ( $\text{S m}^2 \text{ mol}^{-1}$ )	$K_A$ ( $\text{dm}^3 \text{ mol}^{-1}$ )	$R$ ( $\text{\AA}$ )	$\delta$	$\Lambda_0\eta \times 10^4$ ( $\text{S m}^2 \text{ mol}^{-1} \text{ mPa s}$ )	$\text{Ln}(K_A)$	$\Delta G^0$ ( $\text{kJ mol}^{-1}$ )
CH <sub>3</sub> CN	160.59	17.33	12.19	0.51	55.31	2.85	-0.71
CH <sub>3</sub> OH	87.28	73.66	11.82	0.32	47.52	4.30	-1.06
CH <sub>3</sub> NO <sub>2</sub>	84.20	109.96	12.22	0.54	51.70	4.70	-1.16
H <sub>2</sub> O	48.65	225.69	10.85	0.27	43.31	5.42	-1.34
HCONH <sub>2</sub>	27.91	392.90	11.79	0.16	92.15	5.97	-1.48

**Table VI.5. Limiting ionic conductance ( $\lambda_o^\pm$ ), ionic Walden product ( $\lambda_o^\pm\eta$ ), Stokes' radii ( $r_s$ ) and crystallographic radii ( $r_c$ ) of [Bu<sub>4</sub>PMS] in different studied solvents at  $T = 298.15$  K**

Solvents	Ion	$\lambda_o^\pm$ (S m <sup>2</sup> mol <sup>-1</sup> )	$\lambda_o^\pm\eta$ (S m <sup>2</sup> mol <sup>-1</sup> mPa s)	$r_s$ (Å)	${}^b r_c$ (Å)
CH <sub>3</sub> CN	Bu <sub>4</sub> P <sup>+</sup>	62.68	21.59	5.57	4.42
	MS <sup>-</sup>	97.90	33.72	3.50	2.83
CH <sub>3</sub> OH	Bu <sub>4</sub> P <sup>+</sup>	34.07	18.55	4.60	4.42
	MS <sup>-</sup>	53.21	28.97	2.89	2.83
CH <sub>3</sub> NO <sub>2</sub>	Bu <sub>4</sub> P <sup>+</sup>	32.87	20.18	4.06	4.42
	MS <sup>-</sup>	51.33	31.52	2.56	2.83
H <sub>2</sub> O	Bu <sub>4</sub> P <sup>+</sup>	18.99	16.91	3.67	4.42
	MS <sup>-</sup>	29.66	26.41	2.31	2.83
HCONH <sub>2</sub>	Bu <sub>4</sub> P <sup>+</sup>	10.89	35.97	4.73	4.42
	MS <sup>-</sup>	17.01	56.18	2.98	2.83

<sup>b</sup>Crystallographic radii for cation from ref.35 and for anion calculated and judged from Ref.36 respectively.

**Table VI.6: Diffusion coefficient ( $D_{\pm}$ ) and ionic mobility ( $i_{\pm}$ ) of  $\text{Bu}_4\text{P}^+$  and  $\text{MS}^-$  in different studied solvents at 298.15K**

Solvents	$D_{\pm} \cdot 10^{16}/(\text{m}^2 \text{s}^{-1})$		$i_{\pm} \cdot 10^{14}/(\text{m}^2 \text{s}^{-1} \text{volt}^{-1})$	
	$\text{Bu}_4\text{P}^+$	$\text{MS}^-$	$\text{Bu}_4\text{P}^+$	$\text{MS}^-$
$\text{CH}_3\text{CN}$	16.70	26.08	6.50	10.15
$\text{CH}_3\text{OH}$	9.08	14.17	3.53	5.52
$\text{CH}_3\text{NO}_2$	8.76	13.67	3.41	5.32
$\text{H}_2\text{O}$	5.06	7.90	1.97	3.08
$\text{HCONH}_2$	2.90	4.53	1.13	1.76

**Table VI.7: Stretching frequencies of the functional groups present in the solvents and change of frequency after addition of IL, [Bu<sub>4</sub>PMS] in the solvents.**

Stretching frequencies					
Solvents	Functional Group	Range (v cm <sup>-1</sup> )	Pure Solvent (v <sub>o</sub> cm <sup>-1</sup> )	[Bu <sub>4</sub> PMS]+Solvent (v <sub>s</sub> cm <sup>-1</sup> )	Δv (cm <sup>-1</sup> )
CH <sub>3</sub> CN	C≡N	2210-2260	2255.6	2289.4	33.8
	C-H	2850-2950	2917.2	2920.6	3.4
CH <sub>3</sub> OH	O-H	3200-3600	3384.7	3426.6	41.9
	C-H	2850-2950	2918.9	2921.3	2.4
CH <sub>3</sub> NO <sub>2</sub>	N-O	1500-1570 (v <sub>as</sub> )	1565.3 (v <sub>as</sub> )	1617.9 (v <sub>as</sub> )	52.6
		1300-1370 (v <sub>s</sub> )	1363.8 (v <sub>s</sub> )	1414.8 (v <sub>s</sub> )	51.0
	C-H	2850-2950	2963.0 (v <sub>as</sub> ) 2872.9 (v <sub>s</sub> )	2964.4 (v <sub>as</sub> ) 2873.5 (v <sub>s</sub> )	1.4 0.6
H <sub>2</sub> O	O-H	3100-3800	3449.2 (v <sub>as</sub> )	3514.8 (v <sub>as</sub> )	65.6
			3344.6 (v <sub>s</sub> )	3405.1 (v <sub>s</sub> )	60.5
HCONH <sub>2</sub>	N-H	1500-1600	1578.7	1589.9	11.2
	C=O	1650-1695	1693.4	1782.6	89.2
	C-N	~1400	1402.0	1403.5	1.5

## FIGURES

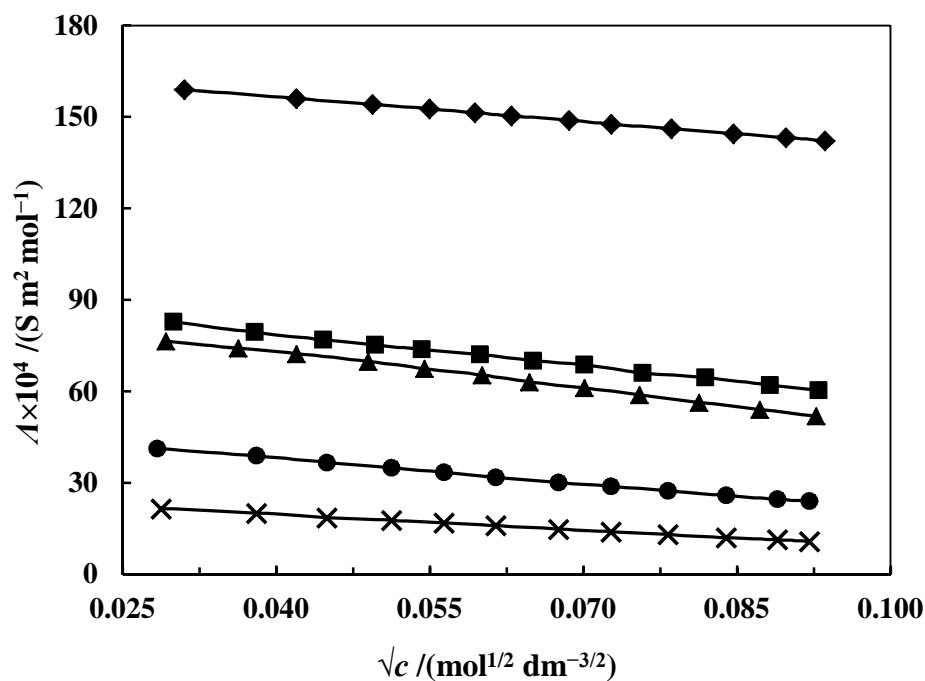


**Figure VI.1:** Plot of molar conductance ( $\Lambda$ ) and the square root of molar concentration ( $\sqrt{c}$ ) of  $\text{Bu}_4\text{PMS}$  in  $\text{CH}_3\text{CN}$  (◆),  $\text{CH}_3\text{OH}$  (■),  $\text{CH}_3\text{NO}_2$  (▲),  $\text{H}_2\text{O}$  (●), and  $\text{HCONH}_2$  (×) respectively at  $T = 298.15\text{K}$

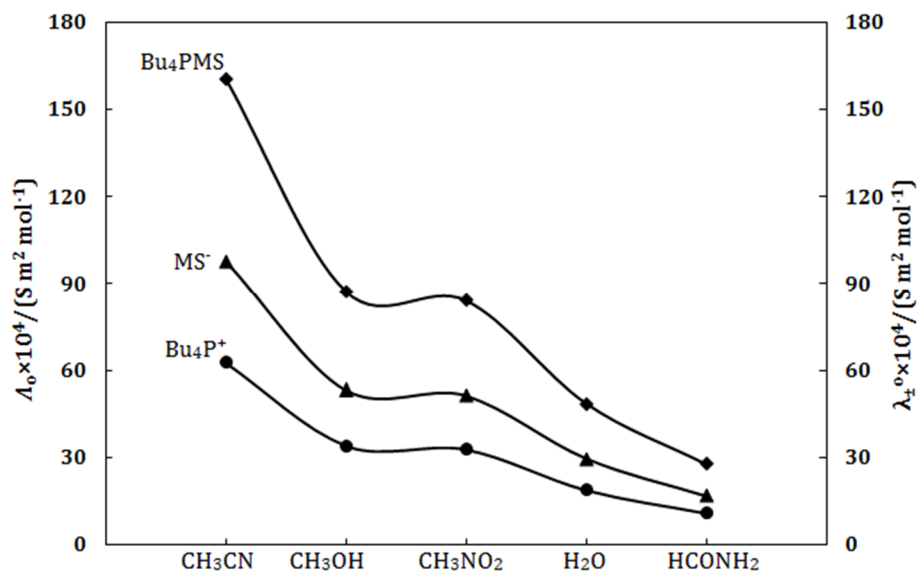
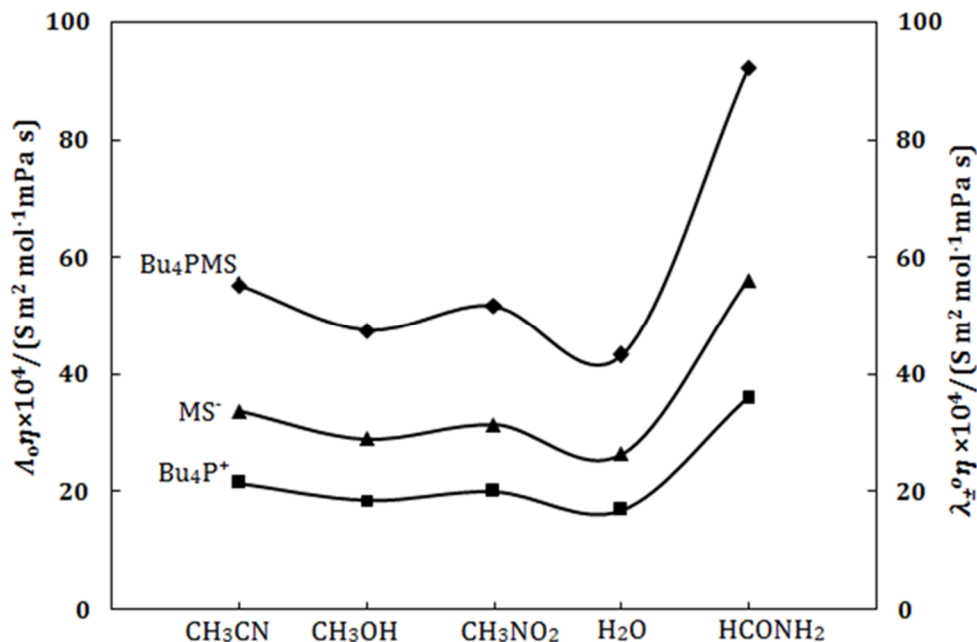


**Figure VI.2:** Plot of limiting molar conductance ( $\Lambda_0$ ) for  $\text{Bu}_4\text{PMS}$  (◆), and limiting ionic conductance for  $\text{Bu}_4\text{P}^+$  (●),  $\text{MS}^-$  (▲) in different studied solvents at  $T = 298.15\text{K}$



Product ( $\lambda_{\circ}^{\pm}\eta$ ) for Bu<sub>4</sub>P<sup>+</sup> (●), MS<sup>-</sup> (▲) in different studied solvents at  $T = 298.15\text{K}$

**Figure VII.3:** Plot of Walden Product ( $\Lambda_0\eta$ ) for Bu<sub>4</sub>PMS (◆), and ionic Walden

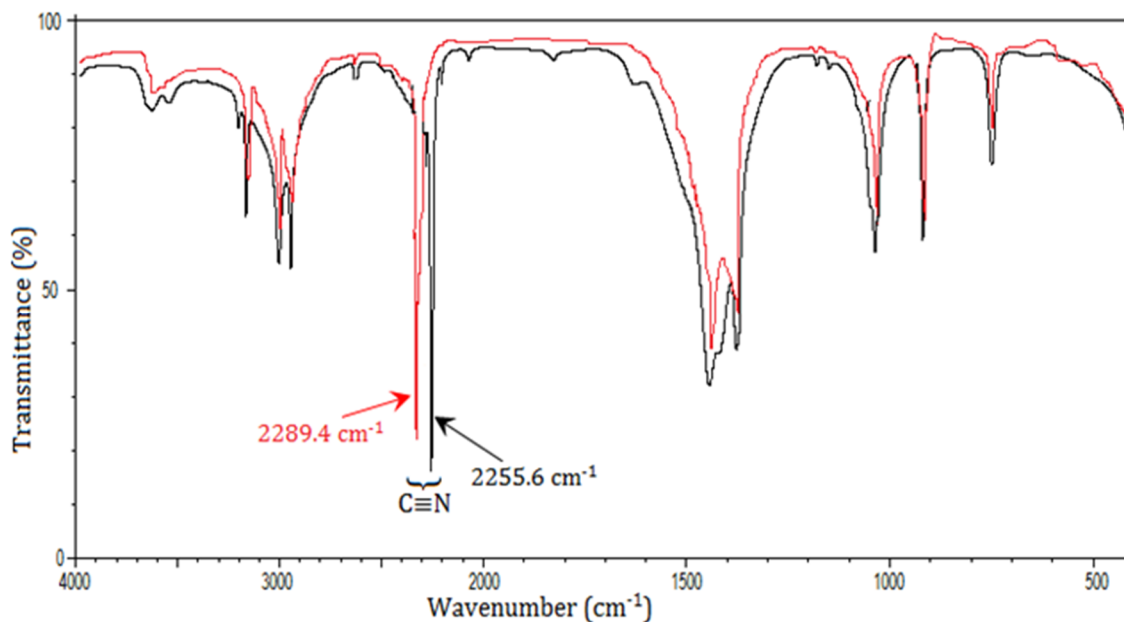


**Figure VII.4:** Stretching frequency of C≡N in acetonitrile (black solid line) and in {[Bu<sub>4</sub>PMS]+CH<sub>3</sub>CN} (red solid line)

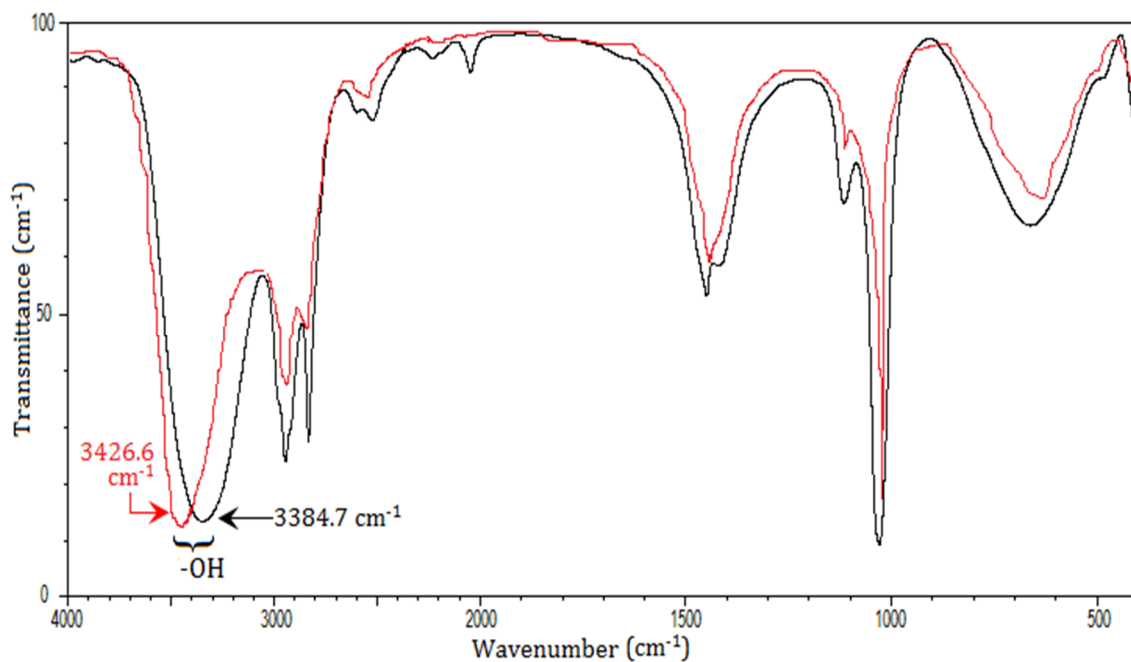


**Figure VII.5:** Stretching frequency of O-H in methanol (black solid line) and in  $\{[\text{Bu}_4\text{PMS}]+\text{CH}_3\text{OH}\}$  (red solid line)

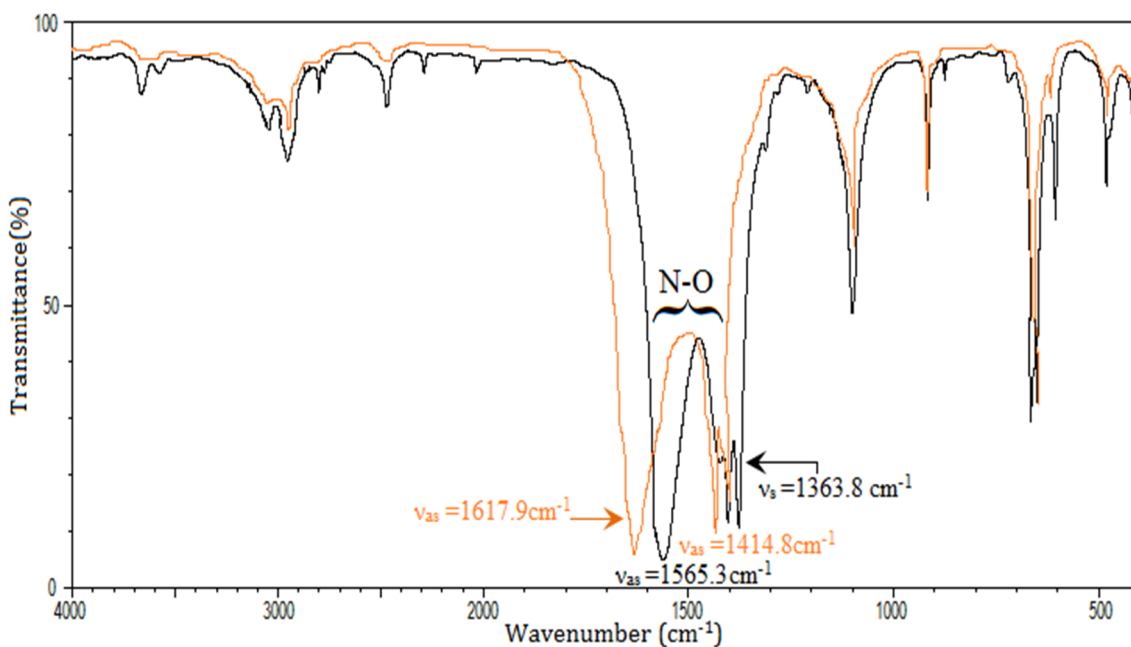


**Figure VII.6:** Stretching frequency of N-O in nitromethane (black solid line) and in  $\{[\text{Bu}_4\text{PMS}]+\text{CH}_3\text{NO}_2\}$  (red solid line)

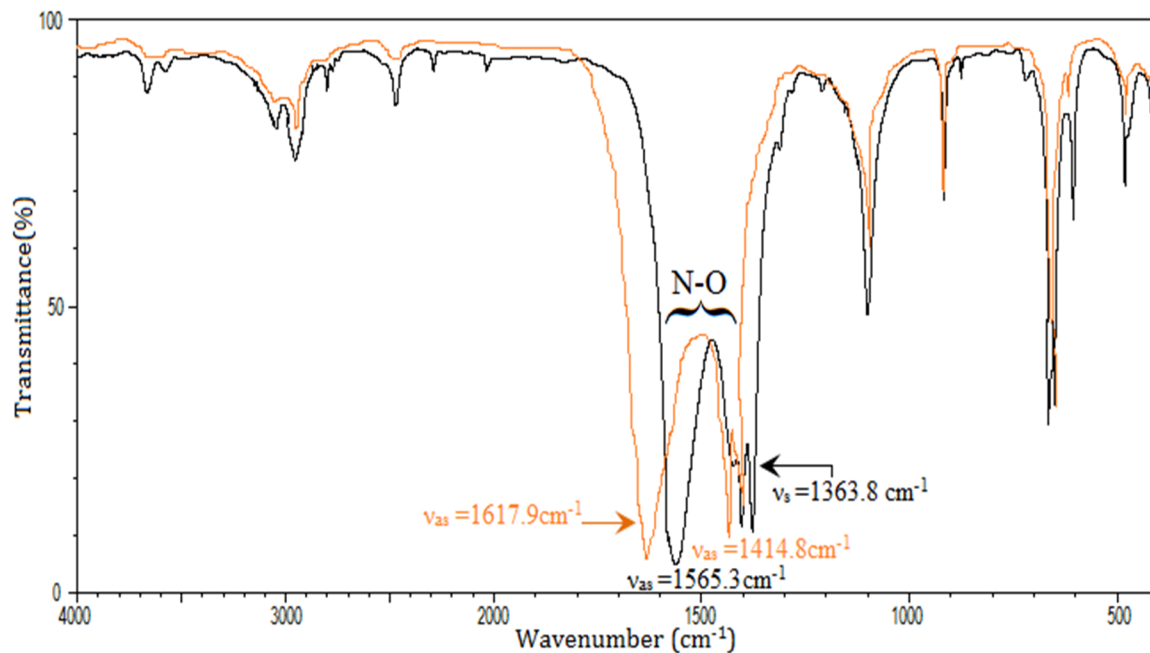


**Figure VII.7:** Stretching frequency of O-H in water (black solid line) and in  $\{[\text{Bu}_4\text{PMS}] + \text{H}_2\text{O}\}$  (red solid line)

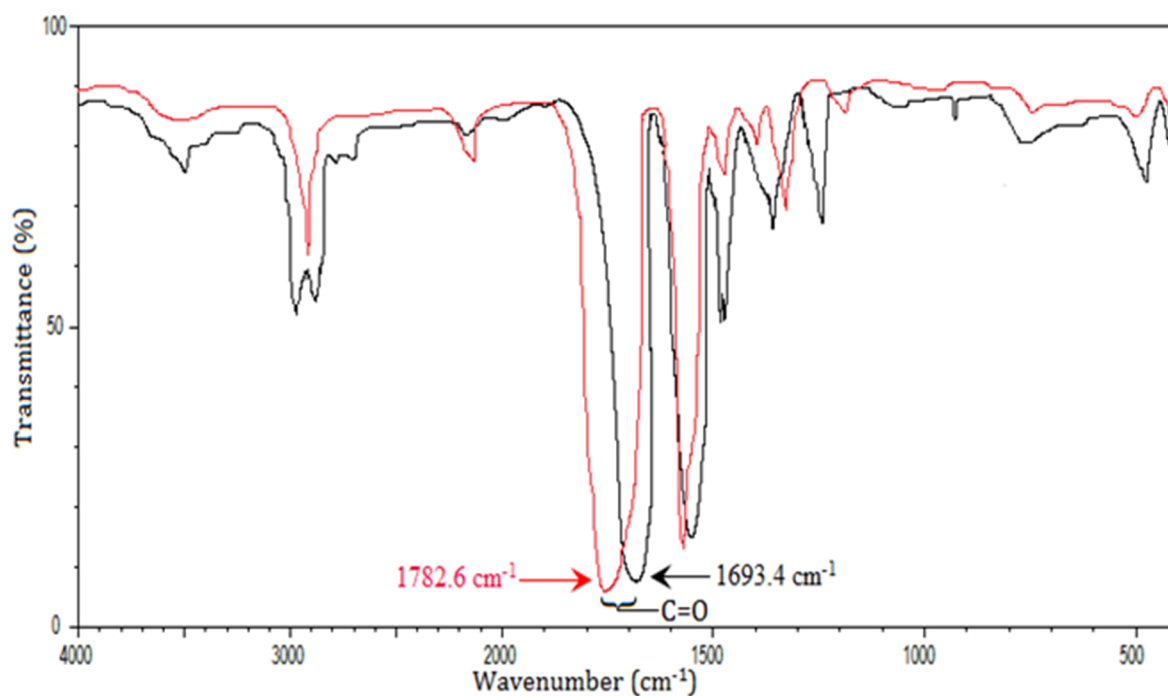
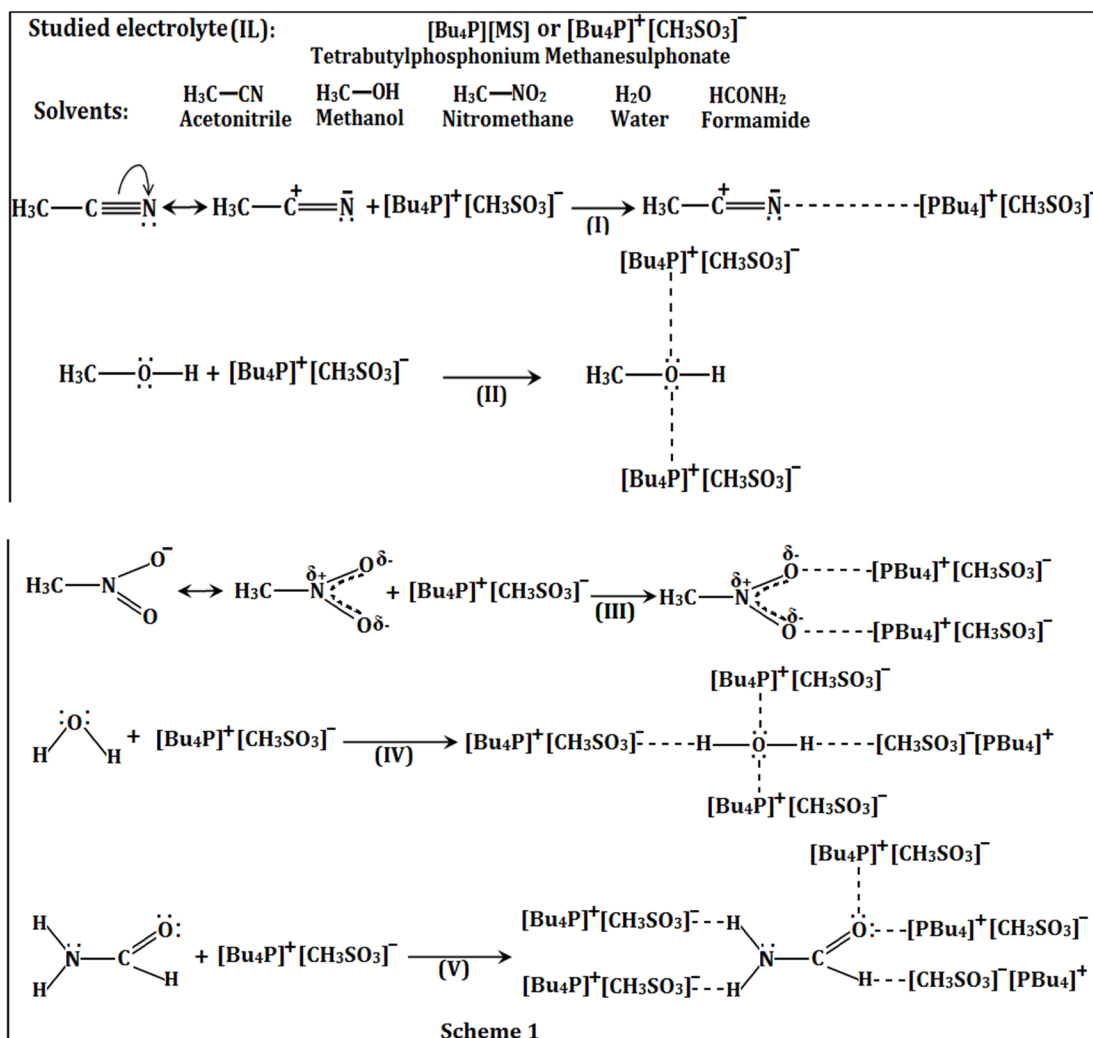
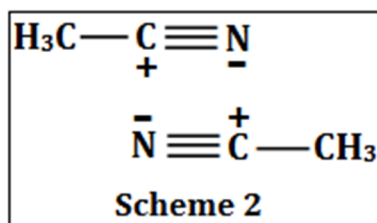


**Figure VII.8:** Stretching frequency of C=O in formamide (black solid line) and in  $\{[\text{Bu}_4\text{PMS}] + \text{HCONH}_2\}$  (red solid line)

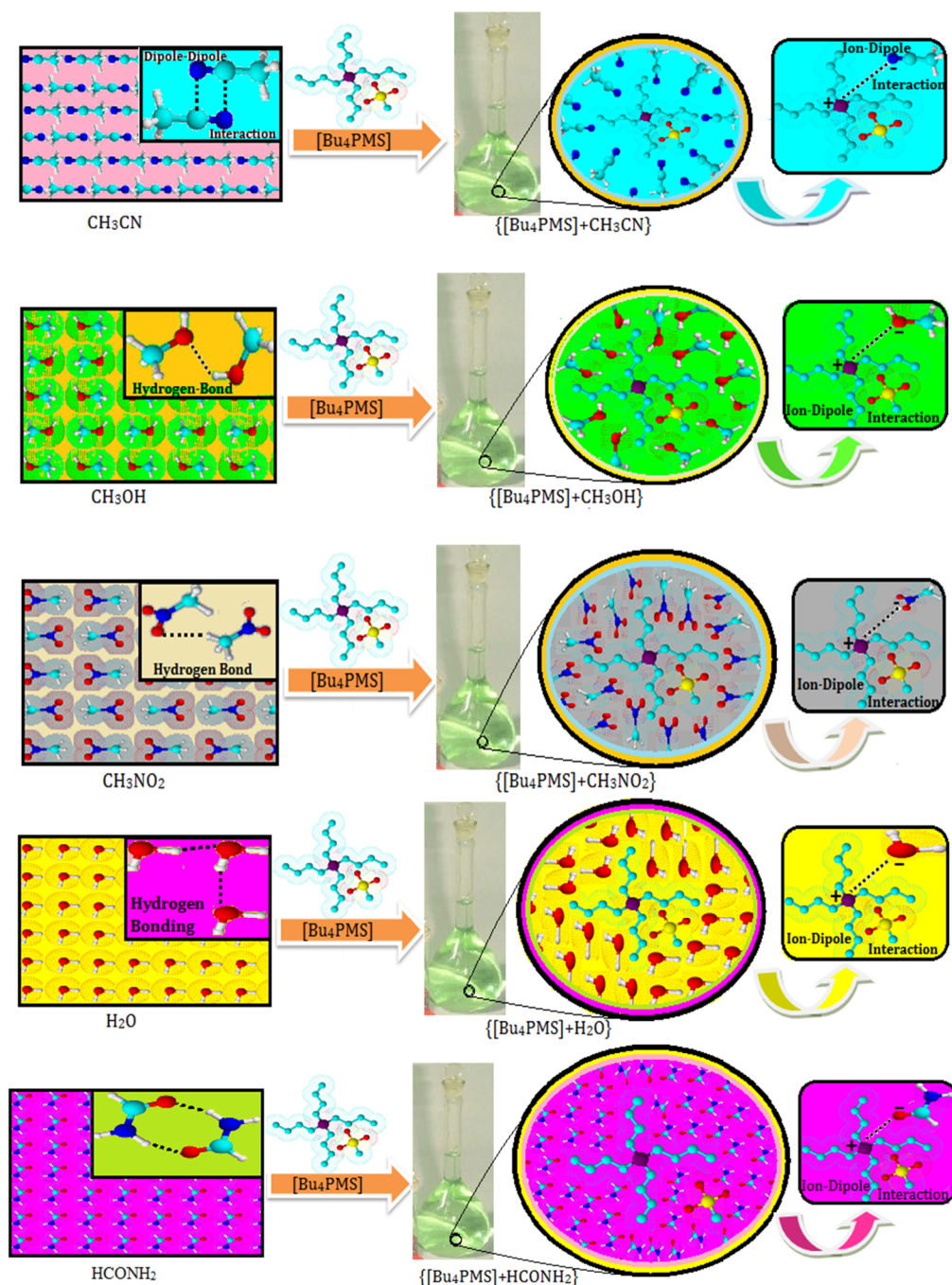
## SCHEMES



**Scheme VII.1:** The schematic representation of ion-solvation, for the particular ion in the studied solutions {[Bu<sub>4</sub>PMS]+solvents}



**Scheme VII.2:** Antiparallel dimerization of acetonitrile (CH<sub>3</sub>CN)



**Scheme 3**

**Scheme VII.3:** Schematic representation of the interaction occurring in pure solvent and {[EMIm]Br+Solvent} together with the trend in the ion-solvation in the studied solvents which is as follows: **CH<sub>3</sub>CN < CH<sub>3</sub>OH < CH<sub>3</sub>NO<sub>2</sub> < H<sub>2</sub>O < HCONH<sub>2</sub>**